UNIVERSITY OF ZIELONA GÓRA

CIVIL AND ENVIRONMENTAL ENGINEERING REPORTS

E-ISSN 2450-8594

CEER 2024; 34 (4): 0293-0306
DOI: 10.59440/ceer/195601

Original Research Article

OPTIMAL DESIGN OF RECTANGULAR TANK WALLS WITH RIBS USING NUMERICAL MODELS AND GLOBAL OPTIMIZATION

Tomasz GARBOWSKI[1], Przemysław BORECKI[1], Janusz RUTKOWSKI[1], Anna SZYMCZAK-GRACZYK[2]

[1]Department of Biosystems Engineering, Poznan University of Life Sciences, Poland
[2]Department of Construction and Geoengineering, Poznan University of Life Sciences, Poland

A b s t r a c t

This paper addresses the optimization of the cross-section in rectangular above-ground tank walls, incorporating vertical ribs and an optional top ring. The objective is to minimize the volume of concrete used, while maintaining key performance criteria such as keeping the maximum tensile stress below the material's allowable limit and minimizing deflections. The analysis is performed using the finite element method (FEM), with the optimization handled through a local gradient-based algorithm (trust region method), supported by a multistart technique to navigate the complexity of the design space and avoid suboptimal solutions. The results demonstrate that this approach effectively reduces concrete consumption without exceeding the tensile stress limits or causing excessive deflection, offering more efficient and cost-effective designs for rectangular tanks used in water storage applications. This method provides valuable insights into the balance between material usage and performance constraints, contributing to sustainable engineering practices.

Keywords: rectangular concrete tanks with ribs, cross-section optimization, finite element method, trust region algorithm, multistart optimization

1. INTRODUCTION

Effective water management is becoming increasingly important as extreme weather events like droughts and floods impact both urban and rural areas. These events necessitate the development of robust infrastructure, particularly storage tanks, which play a critical role in water management systems and the storage of materials from technological processes [1,2]. Tanks can be made from various materials, including steel, concrete, and plastic. Standardized designs are more common for steel and plastic tanks, often pre-fabricated and ready for assembly on delivery. This has significantly advanced

[2] Corresponding author: Anna Szymczak-Graczyk, Poznan University of Life Sciences, Faculty of Environmental and Mechanical Engineering, Department of Construction and Geoengineering, Piątkowska Street 94, 60-649 Poznań, e-mail: anna.szymczak-graczyk@up.poznan.pl, phone: +48602516345

the design of small-capacity tanks for water [3], gas [4], and bulk materials [5], making them easier to procure and install without the need for administrative permits. These improvements have facilitated better storage solutions for water, grain, waste, and other materials. Plastic and composite tanks, typically used in smaller applications such as wastewater collection or water storage, have also benefitted from these advances [6].

Historically, cooling-tower shell research has evolved from addressing short-term stability to focusing on long-term durability and performance. Early foundational work by Mang and Cedolin [7] utilized modified Hamilton's principle to derive equations for nonlinear dynamic analysis, effectively handling follower loads and seismic responses, a milestone in adapting finite element methods for large structures like cooling towers. As research progressed, Bamu and Zingoni [8] documented the shift towards studying deterioration and structural integrity over time, emphasizing the role of cracking and imperfections. Wen-da and Hao-zhong [9] contributed by refining linear pre-buckling analysis for ring-stiffened shells, showing its practical precision for predicting critical loads. Mang et al. [10] further applied variational principles to model deformation and stability with finite elements, aligning empirical stability measures with calculated safety margins. Collectively, these studies have deeply influenced modern strategies in cooling-tower shell analysis, bridging theoretical rigor with practical durability considerations.

Designing tanks requires a comprehensive understanding of static analysis and the interrelationship of different elements. Traditional methods often treat rectangular tanks as combinations of separate plates, such as the wall, base, and cover plates. For tanks with rectangular cross-sections, if the differences in calculated moments are within 10%, the higher value is typically used. In cases of larger discrepancies, techniques like the Cross method are employed to distribute the moments according to plate stiffness [11,12]. Concrete tanks, especially larger ones, present greater design complexity due to the challenge of ensuring watertight joints between prefabricated elements. However, many large concrete tanks are custom-designed to meet the specific requirements of the investor and the operational needs of the stored materials. Concrete remains a popular construction material for tanks due to its durability, with recent advances in protective technologies improving its resistance to aggressive substances stored inside tanks [13,14].

Most tanks are constructed with walls of constant thickness. However, research has demonstrated that walls with a trapezoidal cross-section, where the thickness increases with depth, better optimize the load-bearing capacity of the structure. This is particularly effective in structures subjected to hydrostatic pressure, where the load increases with depth, justifying thicker walls at the bottom. These designs result in material savings and better performance, although they present construction challenges [15]. Despite these benefits, the majority of literature still focuses on tanks with uniform wall thickness [16,17], covering guidelines for correct design and methods for correcting errors [11,12].

Tanks are subjected to various loads, including permanent loads like self-weight and backfill pressure, as well as variable loads such as snow, vehicular traffic, earth pressure, and friction. Temperature-induced loads are often less discussed, though they can cause substantial stresses, particularly when temperature differences between wall surfaces induce bending moments, which increase proportionally to the square of the wall thickness [18]. As a result, thinner upper walls, which are more exposed to temperature effects, are often more appropriate. There remains relatively little research on tanks with variable wall thickness, particularly in the context of temperature-induced stress [19,20].

Several studies [15,21] have demonstrated the benefits of designing tanks with variable wall thickness under thermal and hydrostatic loads. Numerical simulations of plates with variable thickness subjected to temperature effects have shown that these designs result in better performance under both load conditions. Additionally, experiments have validated the efficiency of these designs, showing that

tanks with trapezoidal wall cross-sections distribute internal forces more efficiently, leading to material savings [15].

In recent years, there has been growing interest in advanced numerical techniques for optimizing the design and performance of concrete structures, especially composite and prefabricated systems. The use of numerical homogenization methods has emerged as a powerful approach for accurately modeling the mechanical behavior of multi-layered and complex materials, such as concrete slabs. Studies have demonstrated the effectiveness of combining solid truss and shell elements for homogenization, particularly when dealing with prefabricated composite slabs. This allows for significant improvements in both accuracy and computational efficiency when analyzing the structural performance of large-scale systems [22,23].

Moreover, recent work has expanded the application of these techniques to include sensitivity analysis and the optimization of composite slabs, such as bubble deck systems, which incorporate voids or hollow sections to reduce weight without compromising strength. The incorporation of nonlinear constitutive laws further enhances the accuracy of these analyses, making them invaluable in optimizing the design and material usage of modern concrete structures. These studies provide a foundation for applying numerical homogenization to various structural elements, and their findings have directly influenced the approach taken in this research [24–26].

While this study focuses on the optimization of structural components in rectangular tank designs, recent advances in optimizing concrete compositions, such as the work by Azmakan et al. [27] on alkali-activated slag concrete, highlight the importance of material durability in challenging environments. Their investigation into the optimal quantities of metakaolin and silica fume for acid-resistant concrete underscores the relevance of material choices when designing long-lasting structures under various environmental stresses . This broader context of material optimization supports the need for ongoing research into both the structural and compositional aspects of concrete design.

In our previous work, we explored the influence of geometric parameters on the internal forces in rectangular tanks with both constant and variable wall thicknesses [28]. It was demonstrated that the use of variable wall thickness, particularly trapezoidal sections, can significantly reduce bending moments at the base of the walls, where the highest stresses occur due to hydrostatic pressure. This results in a more efficient distribution of material, leading to both structural and economic benefits. We also applied numerical optimization methods, including trust region algorithms, to further refine the wall design, focusing on reducing material usage while ensuring that the maximum tensile stresses remain below allowable limits [29]. These optimizations have shown the potential for material savings of 10-15% when compared to traditional designs.

Building on these previous studies, the aim of this paper is to further optimize the design of rectangular above-ground tank walls by employing the finite element method (FEM) coupled with a local gradient-based algorithm (again trust region) but enhanced with multistart techniques. The objective is to minimize the volume of concrete used while keeping tensile stresses below critical limits and minimizing deflections, all of which are treated as boundary conditions. Unlike our previous work, which focused primarily on basic geometric parameters and simplified algorithms, this study focuses on the combined use of FEM and trust region optimization to achieve more refined and practical design solutions. By allowing the cross-section of the wall to vary along its height and considering the effects of vertical ribs and an optional top ring, this work aims to provide new insights into the material efficiency and structural performance of tanks subjected to hydrostatic pressure.

2. NUMERICAL METHODS

This study focuses on optimizing the cross-sectional design of rectangular above-ground tank walls using a combination of the finite element method (FEM) and gradient-based optimization techniques. The aim is to minimize the volume of concrete required while ensuring that the tensile stress remains below allowable limits and deflections are minimized. The primary components of the method are described as follows.

2.1. Finite Element Modelling (FEM)

The structural analysis of the rectangular tanks is performed using the finite element method (FEM). This method is particularly suited to modelling complex geometries and capturing the variations in stress distributions caused by hydrostatic pressure. The tank wall is modelled with variable cross-sectional geometry, allowing for different thicknesses at the top and bottom to account for changes in hydrostatic pressure. Additionally, vertical stiffening ribs are incorporated into the model to enhance structural performance.

For the finite element analysis, planar S4 shell elements were implemented in MATLAB [30] and used in this study. These are four-node, fully integrated shell elements, which provide accurate modelling of the wall behaviour under hydrostatic pressure. Additionally, strip-type elements (linear stiffeners modelled as beam elements) were used to represent the vertical stiffeners. These strip elements share nodes with the shell elements at the stiffener locations, ensuring proper interaction between the wall and the stiffeners. Both the shell elements and the beam elements representing the stiffeners are designed to have variable cross-sections. Specifically, the shell elements can vary in thickness along the wall height, and the cross-sectional properties of the beam elements can change along the length of the stiffeners.

2.2. Geometry and Boundary Conditions

The geometry of the tank walls is rectangular, and the thickness of the walls, as already mentioned, is allowed to vary along their height. At the base, the wall is thicker to handle higher hydrostatic pressures, while at the top, the wall is thinner due to reduced pressure. Vertical ribs are placed along the walls to improve load distribution and minimize deflections. The tank may also include an optional top ring to provide additional stiffness near the upper edge.

Boundary conditions are applied to simulate the tank being fully filled with liquid, which generates hydrostatic pressure increasing with depth. The pressure is modelled as a linearly distributed load acting perpendicular to the walls. The bottom of the tank is fixed, and constraints are applied to ensure that the maximum tensile stress remains below the allowable stress for the concrete.

3. MATERIAL MODEL

In this study, the concrete used for the tank walls is modelled as an elastic, isotropic material. Concrete is a complex material that exhibits nonlinear behaviour under loading, especially in tension, but for the purposes of this study, an elastic approximation is applied to capture the material's response under service conditions. The model is supplemented with the Lee-Fenves failure criterion to account for the potential for cracking and material degradation under tensile and compressive stresses, but only in the initiation phase, not during propagation, as we are primarily interested in the onset of failure and the critical stress, rather than the complete failure of the concrete cross-section. Reinforcement was not included in the model used in this study to focus on the primary behaviour of plain concrete under

loading conditions, isolating the fundamental effects of geometry and load application without the complexity introduced by reinforcement interactions.

3.1. Elastic Isotropic Behaviour

Concrete is treated as an elastic isotropic material, meaning that its mechanical properties—modulus of elasticity and Poisson's ratio—are assumed to be uniform in all directions. This simplification allows for easier integration with the finite element method (FEM), while still providing reasonable accuracy for predicting the stress-strain behaviour of the tank walls under hydrostatic pressure.

The key parameters for the elastic material model are:

- Young's Modulus (E): describes the stiffness of the concrete and is used to calculate the stress-strain relationship. The value of E is typically assumed for tanks as 30 MPa.
- Poisson's Ratio (ν): this parameter defines the ratio of transverse to axial strain and is typically small for concrete, assumed here 0.2.

The stress-strain relationship for shells in the elastic regime follows Hooke's Law for isotropic materials:

$$\begin{bmatrix}\sigma_x\\ \sigma_y\\ \tau_{xy}\end{bmatrix} = \frac{E}{1-\nu^2}\begin{bmatrix}1 & \nu & 0\\ \nu & 1 & 0\\ 0 & 0 & \dfrac{1-\nu}{2}\end{bmatrix} = \begin{bmatrix}\varepsilon_x\\ \varepsilon_y\\ \gamma_{xy}\end{bmatrix} \tag{3.1}$$

Where:

- σ_x and σ_y are the normal stresses in the x and y directions, respectively.
- τ_{xy} is the shear stress in the xy-plane.
- ε_x and ε_y are the normal strains in the x and y directions, respectively.
- γ_{xy} is the engineering shear strain in the xy-plane.
- E is Young's modulus (modulus of elasticity).
- ν is Poisson's ratio.

3.2. Lee-Fenves Damage Model

To capture the nonlinear failure behaviour of concrete under stress, the Lee-Fenves damage model [31] is used. This model is widely recognized for its ability to represent the complex behaviour of concrete under tension and compression, accounting for both stiffness degradation and inelastic deformation as damage progresses.

The Lee-Fenves model is based on the following principles [32,33]:

- Cracking under tension: when concrete is subjected to tensile stresses that exceed a critical threshold, it begins to crack. The model tracks this damage and progressively reduces the stiffness of the material to reflect the formation of cracks.
- Crushing under compression: under compressive stresses, concrete experiences crushing at high stress levels. The model accounts for this by reducing the material's stiffness in compression as damage accumulates.
- Biaxial behaviour: the model also captures the different responses of concrete under biaxial stress conditions, where tension in one direction and compression in another can lead to complex failure modes.

The failure criterion is expressed as a function of the equivalent stress and strain, and is characterized by two damage variables: one for tension and one for compression. These variables are updated at each step of the analysis to reflect the current damage state of the material.
The governing equations for the Lee-Fenves model are based on:

$$d_t = d_t(f_t, f_t^*) \quad \text{(for tension)} \tag{3.2}$$

$$d_c = d_c(f_c, f_c^*) \quad \text{(for compression)} \tag{3.3}$$

Where:

- d_t and d_c represent the damage variables in tension and compression, respectively.
- f_t is the current tensile stress, and f_c is the current compressive stress.
- f_t^* is the **peak tensile strength**, representing the maximum tensile stress the concrete can withstand before cracking initiates.
- f_c^* is the **peak compressive strength**, representing the maximum compressive stress before concrete begins to crush.

In these equations, the peak stress values f_t^* and f_c^* define the critical limits for concrete's tensile and compressive strength. Once the stress reaches these peak values, the damage variables d_t and d_c begin to increase, indicating the initiation of cracking and crushing, respectively. However, since the focus of this study is on the initiation phase of failure and the critical stresses, the model does not account for the full propagation of cracks or crushing beyond these initial stages.

3.3. Implementation in FEM

The material model is integrated into the FEM framework to simulate the behaviour of the tank walls under the applied loads. The elastic isotropic model handles the initial elastic response, while the Lee-Fenves failure criterion monitors the onset of damage and progressively adjusts the material properties as cracking or crushing occurs.

This approach allows for a realistic simulation of the concrete's behaviour, particularly in areas where tensile stresses may lead to cracking due to hydrostatic pressure. The integration of this failure model is critical for ensuring that the optimization process remains within the allowable stress limits and does not compromise the structural integrity of the tank walls.

4. OPTIMIZATION STRATEGY

The optimization process is based on minimizing the volume of concrete used in the tank's construction. This is achieved through the use of a local gradient-based optimization algorithm known as the trust region method. The trust region algorithm iteratively searches for the optimal solution by approximating the behaviour of the objective function (concrete volume) within a specified region. This method is well-suited for problems where the design space is highly non-linear, as is the case with variable wall thicknesses and stiffening ribs.

4.1. Multistart Optimization

To avoid being trapped in local minima, the optimization process employs a multistart technique [34]. This approach involves running multiple optimization trials from different starting points in the design space. By initializing the optimization process from various points, the method explores a broader range of potential solutions, increasing the likelihood of finding the global optimum [35,36].

4.2. Objective Function

The objective of the optimization is to minimize the total volume of concrete, which is expressed as:

$$V = \int_A h(x, y) dA \tag{4.1}$$

Where V is the volume of concrete, $h(x, y)$ is the local wall thickness as a function of position on the wall, and A is the total surface area of the wall.

4.3. Design Variables and Constraints

The primary design variables include the thickness of the walls at different points (top and bottom), the placement and geometry of the vertical ribs, and the potential inclusion of a top ring. These variables are adjusted during the optimization process to find the configuration that minimizes the concrete volume.

The optimization is subject to the following constraints:

- Tensile stress constraint: the maximum tensile stress must remain below the allowable limit for the material, ensuring the structure's durability.
- Deflection constraint: wall deflections must not exceed the specified value to prevent excessive deformation, which could compromise the tank's structural integrity and operational efficiency.

5. RESULTS

The analysis focused on one vertical wall of the rectangular tank, idealizing the boundary conditions related to the connections at the corners with the adjacent perpendicular walls. In this example, the analysed wall has dimensions of 9 meters in width and 3 meters in height. The stiffening ribs and wall thickness were allowed to vary along the height to optimize material usage and structural performance. The computational model consisted of approximately 3200 degrees of freedom to capture the stress distribution and deflections under hydrostatic pressure. The model and the number of elements used in this example represent a compromise between the accuracy of the results and the computational efficiency, ensuring that the analysis provides reliable insights while maintaining reasonable calculation times.

In the optimization process, the parameters related to the tank wall and stiffening ribs were varied to achieve an optimal design that minimizes the volume of concrete while meeting stress and deflection constraints. The six key parameters considered in the optimization include the thickness of the wall at the top and bottom, the width and height of the vertical ribs, and the dimensions of an optional horizontal rib. These parameters were adjusted within specified bounds, where the wall thickness at the top and bottom ranged from 0.1 to 0.8 meters, while the rib dimensions were similarly constrained to ensure feasible designs.

The GlobalSearch algorithm was employed to guide the optimization process. This method uses a global search strategy, starting from multiple initial points to explore the design space and avoid getting trapped in local minima. The algorithm was set to run with 50 trial points and 40 stage one points, ensuring a broad exploration of potential solutions. As the algorithm iterates, it narrows down the search toward the global optimum by evaluating and refining the design parameters based on the objective function—minimizing the volume of concrete used for the tank wall and ribs.

The stopping criteria for the GlobalSearch algorithm were based on both the convergence of the objective function and the satisfaction of the defined constraints. Specifically, the optimization process

sought to reduce the volume of concrete while ensuring that the maximum tensile stress in the wall remained below 3 MPa. In addition, deflections were minimized to prevent excessive deformation that could affect the tank's structural performance. Once the best solution was found, with no further improvements identified in subsequent iterations, the algorithm stopped. This approach allowed the identification of an optimized design that balances material efficiency with structural integrity.
The FEM analysis is coupled with the optimization algorithm in an iterative process. After each iteration, the FEM model recalculates the stress and deflection distribution for the current configuration of the tank wall. The results are fed back into the optimization algorithm, which adjusts the design variables accordingly. This process continues until the algorithm converges on an optimal solution that satisfies all constraints while minimizing the concrete volume.

Figures 1 and 2 present the distribution of deflections and Huber-Mises-Hencky stresses in the optimized rectangular tank wall, respectively.

Figure 1 shows the deflection results, where the deformation of the tank wall under hydrostatic pressure is captured. The maximum deflection, as expected, occurs near the upper region of the wall, with values reaching approximately 1.70×10^{-3} meters. The deflection decreases toward the bottom, where the wall is thicker and subjected to higher stiffness, with values approaching zero. The distribution reflects the optimized design, where the variable wall thickness effectively reduces deformation while minimizing material usage.

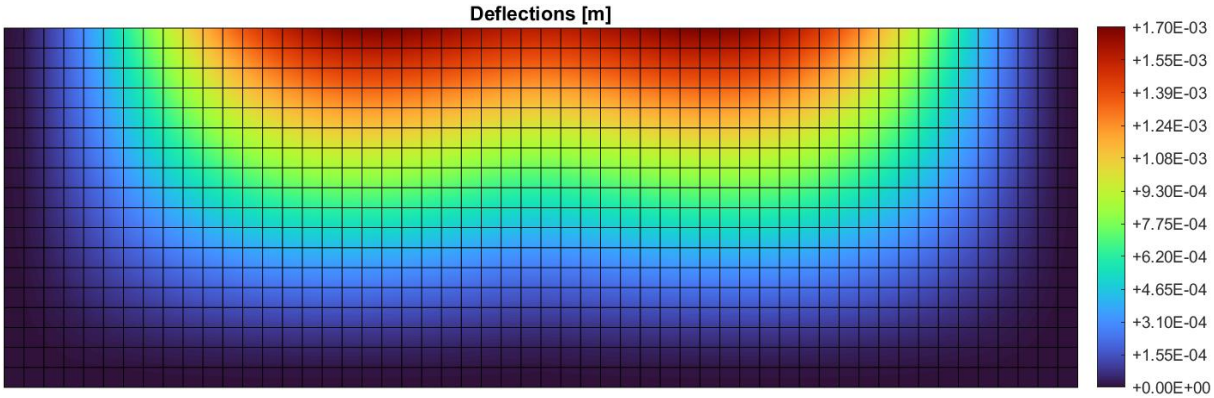

Fig. 1. Distribution of deflections in the optimized rectangular tank wall

Figure 2 presents the Huber-Mises-Hencky stress distribution, which highlights the areas of the wall experiencing the highest stress levels. The maximum Von Mises stress, around 2.67 MPa, occurs in the lower region of the wall, where hydrostatic pressure is greatest. The stresses decrease moving upward, reflecting the reduced hydrostatic pressure toward the top of the tank. The stress concentrations at the corners and near the vertical stiffeners are also visible, demonstrating the effectiveness of the ribs in distributing the stresses and reinforcing the structure.

Together, these figures demonstrate how the design effectively balances deflection and stress distribution while adhering to the material and structural constraints.

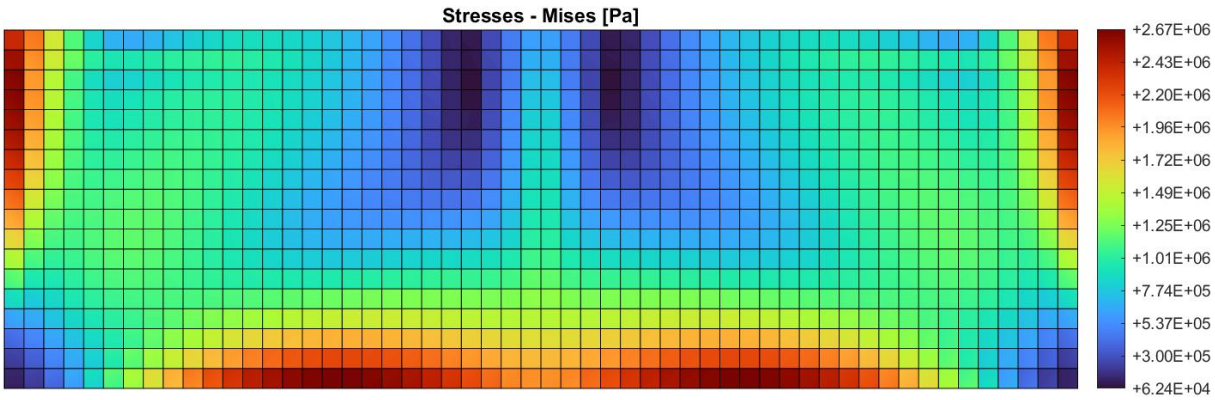

Fig. 2. Distribution of Huber-Mises-Hencky stresses in the optimized rectangular tank wall

Figure 3 illustrates the convergence of the geometric parameters over the course of the optimization process. The parameters include the top and bottom wall thicknesses, rib dimensions (width and height), and the ring width/height. As the iterations progress, there is noticeable variation in the values, especially in the early stages, which reflects the algorithm's exploration of the design space. However, after approximately 250 iterations, the parameters begin to converge to their optimal values, as indicated by the stabilization of the lines near the final iteration. The "best solution" is marked at the point where the parameters reach their final optimized values, demonstrating the efficiency of the multistart optimization approach in finding the best design configuration.

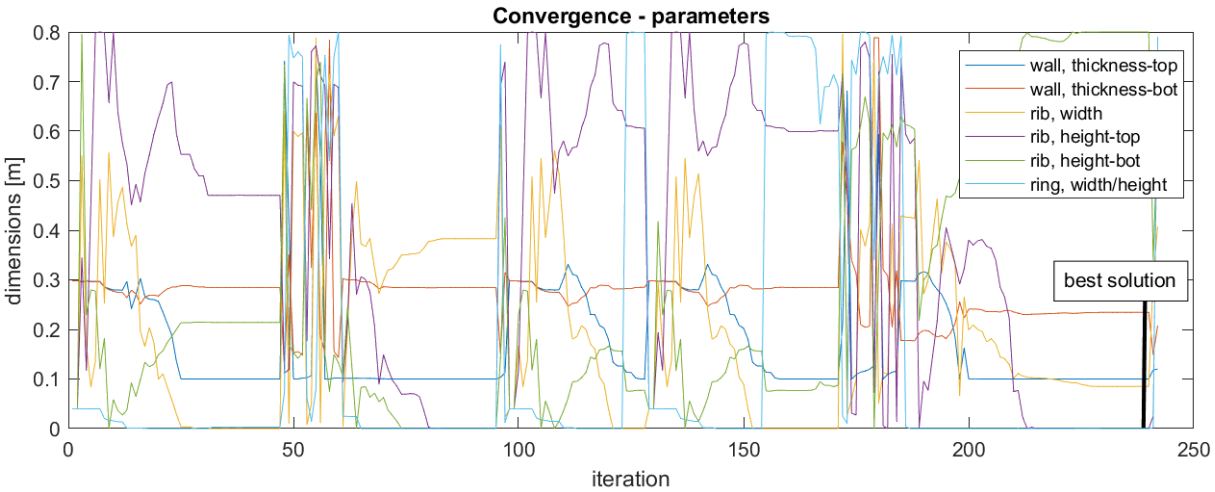

Fig. 3. Convergence of the geometric parameters over the course of the optimization process.

Figure 4 shows the convergence of the objective function, which is the total volume of concrete to be minimized. Initially, the objective function experiences significant fluctuations, reflecting the adjustments made by the optimization algorithm as it searches for an optimal solution. As the iterations progress, the objective function gradually decreases, with noticeable dips indicating substantial improvements in the solution. By around iteration 200, the function stabilizes, converging toward the final optimal solution, where the best design is achieved with minimal concrete volume. The best solution is clearly marked near the end, where the objective function reaches its lowest value.

These figures collectively demonstrate the effectiveness of the optimization process, with Fig. 3 showing the stabilization of design parameters and Fig. 4 confirming the minimization of the objective function, both converging toward an optimal solution.

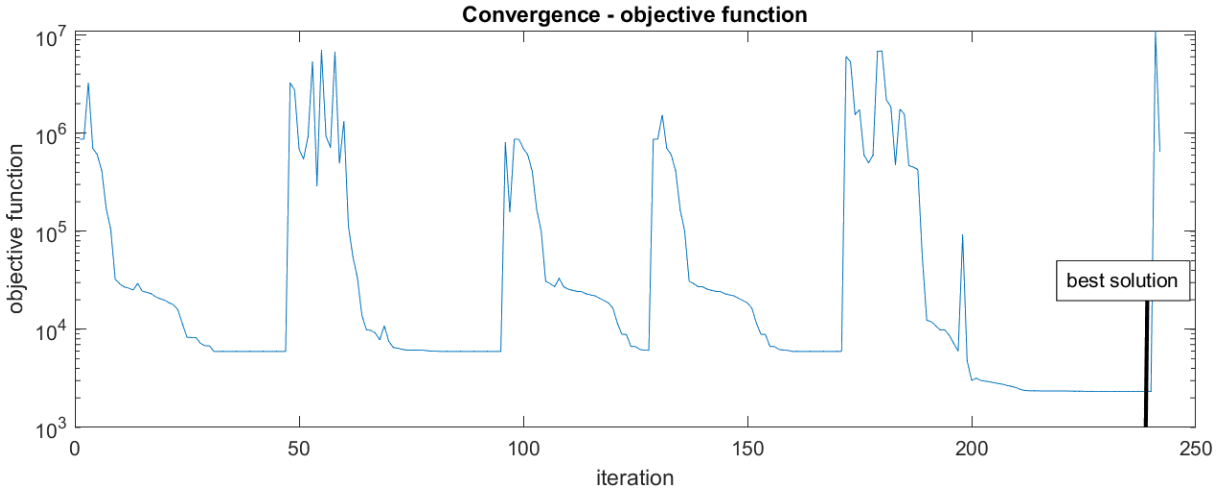

Fig. 4. Convergence of the objective function

Figure 5 presents the optimized configuration of one wall of the rectangular tank, showing the final design after the optimization process. Both the tank wall and the stiffening ribs exhibit varying dimensions along the height, reflecting the structural need to accommodate different stress distributions caused by hydrostatic pressure.

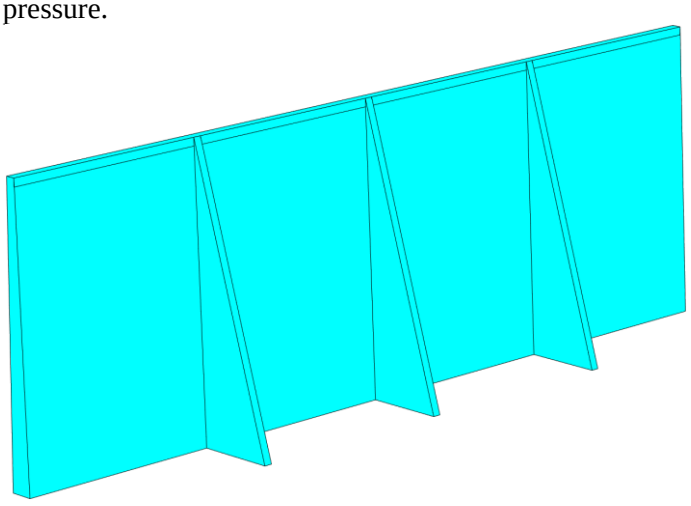

Fig. 5. Optimized configuration of one wall of the rectangular tank

The wall thickness increases toward the bottom, where the pressure is greatest, while it tapers toward the top, where the pressure is lower. Similarly, the stiffening ribs are wider and deeper at the base to provide additional support in the regions subjected to higher loads. At the top, the ribs are more slender, reflecting the reduced structural demand in this region. This variation in geometry demonstrates the effectiveness of the optimization process in balancing material usage with structural performance.

This final configuration represents the most efficient use of concrete material while adhering to the constraints on deflection and tensile stress, ensuring both cost-efficiency and structural integrity. Table 1 presents the starting and final (optimized) dimensions of the wall of tank.

Table 1. The starting and final design parameters.

parameter	Initial value [m]	Optimal value []
Wall thickness at the top	0.20	0.100
Wall thickness at the bottom	0.20	0.234
Width of vertical ribs	0.20	0.085
Height of the rib at the top	0.20	0.000
Height of stiffener at the bottom	0.20	0.800
Width/Height of horizontal stiffener	0.20	0.000

6. DISCUSSION

The optimization results demonstrated a significant improvement in both material efficiency and structural performance. By allowing the wall thickness and rib dimensions to vary along the height of the tank, the final design achieved a more efficient use of concrete, particularly in areas subject to lower stress. The thickening of the wall toward the bottom, where hydrostatic pressure is greatest, ensured that the structural integrity was maintained, while the thinner upper sections contributed to material savings. This distribution reflects the optimization strategy's ability to target regions of high demand with increased material, while reducing unnecessary thickness where it is not required. The ribs, optimized for both width and height, played a crucial role in reducing deflections and distributing the stresses more evenly across the wall. The GlobalSearch algorithm efficiently identified the best configuration by thoroughly exploring the design space, confirming that it is well-suited for this type of structural optimization problem.

The comparison between the initial and final designs clearly highlights the benefits of optimization. In the initial configuration, with uniform thickness and ribs, deflections were significantly higher, particularly near the upper regions of the tank. By contrast, the optimized design showed a marked reduction in deflections, especially in critical areas, thanks to the tailored rib dimensions. The stress analysis also revealed that the optimized design kept the tensile stresses well below the 3 MPa limit, while the material volume was minimized, offering an efficient, cost-effective solution. This balance between structural constraints and material usage illustrates the effectiveness of the adopted approach, particularly for tanks subjected to hydrostatic loads, where the distribution of stresses is non-uniform.

The optimized designs are compared with conventional designs where wall thickness is constant along the height. The effectiveness of the optimization is evaluated by comparing material usage, maximum tensile stresses, and deflections. Previous studies have shown that designs with variable wall thickness can achieve up to 15% material savings while maintaining structural performance [24,25]. The results of this study aim to further validate these findings by demonstrating the effectiveness of the trust region and multistart optimization approaches in the design of rectangular tanks.

7. CONCLUSIONS

This study demonstrated the potential for significant material savings and improved structural performance through the optimization of rectangular tank walls. By employing a GlobalSearch

algorithm to adjust the wall thickness and rib dimensions, we achieved a design that met stringent constraints on tensile stress and deflections while minimizing the volume of concrete used. The optimization process allowed for a variable wall thickness, tailored to the stress distribution caused by hydrostatic pressure, as well as optimized stiffening ribs that improved the tank's resistance to deformation. The results validate the use of advanced optimization techniques in civil engineering, particularly for structures subjected to non-uniform loading conditions, such as storage tanks.

In conclusion, the optimized design presents a practical solution for reducing construction costs without compromising safety or performance. The methodology demonstrated in this study can be further applied to other types of structures where non-uniform stress distributions occur, allowing engineers to design more efficient, cost-effective structures. The proposed method is versatile and can be applied to both above-ground and underground tanks, as well as in aquatic environments. It imposes no restrictions on incorporating additional static and environmental loads, such as temperature effects, making it adaptable to a wide range of design scenarios. Future work could explore additional design parameters or extend this approach to more complex geometries, further improving the application of optimization in structural engineering.

REFERENCES

1. Laks, I, Walczak, Z and Walczak, N 2023. Fuzzy analytical hierarchy process methods in changing the damming level of a small hydropower plant: Case study of Rosko SHP in Poland. *Water Resources and Industry* **29**, 100204. doi: 10.1016/j.wri.2023.100204.
2. Laks, I and Walczak, Z 2020. Efficiency of Polder Modernization for Flood Protection. Case Study of Golina Polder (Poland). *Sustainability* **12**, 8056. doi: 10.3390/su12198056.
3. Ziółko, J 1983. Zbiorniki, silosy [Tanks, silos]. In: Bogucki W (ed) *Poradnik projektanta konstrukcji metalowych: Tom II* [Designer's guide to metal structures: Volume II]. Warszawa: Arkady.
4. Ziółko, J 1986. *Zbiorniki metalowe na ciecze i gazy* [Metal tanks for liquids and gases]. Warszawa: Arkady.
5. Horajski, P, Bohdal, L, Kukielka, L, Patyk, R, Kaldunski, P and Legutko, S 2021. Advanced Structural and Technological Method of Reducing Distortion in Thin-Walled Welded Structures. *Materials* **14**, 504. doi: 10.3390/ma14030504.
6. Buczkowski, W, Mikołajczak, H and Szymczak-Graczyk, A 2005. Przykładowa ocena rozwiązań materiałowo-konstrukcyjnych zbiorników cylindrycznych z żywic poliestrowo-szklanych stosowanych w przydomowych oczyszczalniach ścieków [Example evaluation of material and structural solutions for cylindrical tanks made of polyester-glass resins used in domestic sewage treatment plants]. *Gaz, Woda i Technika Sanitarna* **12**, 25-28.
7. Mang, HA and Cedolin, L 1978. Cooling tower analysis by a finite element technique based on a modified Hamilton's principle. *Meccanica* **13**, 208–224. doi: 10.1007/bf02128387.
8. Bamu, PC and Zingoni, A 2005. Damage, deterioration and the long-term structural performance of cooling-tower shells: A survey of developments over the past 50 years. *Engineering Structures* **27**, 1794–1800. doi: 10.1016/j.engstruct.2005.04.020.
9. Wen-da, L and Hao-zhong, G 1989. Buckling of cooling tower shells with ring-stiffeners. *Applied Mathematics and Mechanics* **10**, 583–592. doi: 10.1007/bf02115790.
10. Mang, H, Gallagher, RH, Cedolin, L and Torzicky, P 1978. Deformation und Stabilität windbeanspruchter Kühlturmschalen. *Ingenieur-Archiv*, **47**, 391–410. doi: 10.1007/bf00538360.
11. Halicka, A and Franczak, D 2011. *Projektowanie zbiorników żelbetowych. Tom 1. Zbiorniki na materiały sypkie* [Design of reinforced concrete tanks. Volume 1. Tanks for bulk materials]. Warszawa: Wydawnictwo Naukowe PWN.

12. Halicka, A and Franczak, D 2014. *Projektowanie zbiorników żelbetowych. Tom 2. Zbiorniki na ciecze* [Design of reinforced concrete tanks. Volume 2. Tanks for liquids]. Warszawa: Wydawnictwo Naukowe PWN.
13. Sybis, M and Konował, E 2022. Influence of Modified Starch Admixtures on Selected Physicochemical Properties of Cement Composites. *Materials* **21**, 7604. doi: 10.3390/ma15217604.
14. Sybis, M, Konował, E and Prochaska, K 2022. Dextrins as green and biodegradable modifiers of physicochemical properties of cement composites. *Energies* **11**, 4115. doi: 10.3390/en15114115.
15. Buczkowski, W, Szymczak-Graczyk, A and Walczak, Z 2017. Experimental validation of numerical static calculations for a monolithic rectangular tank with walls of trapezoidal cross-section. *Bulletin of the Polish Academy of Sciences: Technical Sciences* **65**, 799–804. doi: 10.1515/bpasts-2017-0088.
16. Szymczak-Graczyk, A 2020. Numerical Analysis of the Bottom Thickness of Closed Rectangular Tanks Used as Pontoons. *Applied Sciences* **10**(22), 8082. doi: 10.3390/app10228082.
17. Szymczak-Graczyk, A 2018. Floating platforms made of monolithic closed rectangular tanks. *Bulletin of the Polish Academy of Sciences: Technical Sciences* 66, 209–219. doi: 10.24425/122101.
18. Buczkowski, W and Szymczak-Graczyk, A 2020. Monolityczne zbiorniki prostopadłościenne obciążone temperaturą [Monolithic rectangular tanks subjected to temperature loads]. *Przegląd Budowlany* **9**, 24-29.
19. Buczkowski, W 2008. On reinforcement of temperature loaded rectangular slabs. *Archives of Civil Engineering* 54(2), 315-331.
20. Buczkowski, W, Czajka, S and Pawlak, T 2006. Analiza pracy statycznej zbiornika prostopadłościennego poddanego działaniu temperatury [Static analysis of a rectangular tank subjected to temperature loads]. *Acta Scientiarum Polonorum, Architectura* **5**(2), 17-29.
21. Szymczak-Graczyk, A 2019. Rectangular plates of a trapezoidal cross-section subjected to thermal load. *IOP Conference Series: Materials Science and Engineering* **603**, 032095. doi: 10.1088/1757-899X/603/3/032095.
22. Staszak, N, Garbowski, T and Szymczak-Graczyk, A 2021. Solid Truss to Shell Numerical Homogenization of Prefabricated Composite Slabs. *Materials* **14**, 4120. doi: 10.3390/ma14154120.
23. Staszak, N, Szymczak-Graczyk, A and Garbowski, T 2022. Elastic Analysis of Three-Layer Concrete Slab Based on Numerical Homogenization with an Analytical Shear Correction Factor. *Applied Sciences* **12**, 9918. doi: 10.3390/app12199918.
24. Staszak, N, Garbowski, T and Ksit, B 2023. Optimal Design of Bubble Deck Concrete Slabs: Sensitivity Analysis and Numerical Homogenization. *Materials* **16**, 2320. doi: 10.3390/ma16062320.
25. Staszak, N, Garbowski, T and Ksit, B 2022. Application of the Generalized Nonlinear Constitutive Law in Numerical Analysis of Hollow-Core Slabs. *Archives of Civil Engineering* **68**(2), 125-145. doi: 10.24425/ace.2022.140633.
26. Gajewski, T, Staszak, N and Garbowski, T 2023. Optimal Design of Bubble Deck Concrete Slabs: Serviceability Limit State. *Materials* **16**, 4897. doi: 10.3390/ma16144897.
27. Azmakan, A, Ahmadi, J, Shahani, A, Badarloo, B and Garbowski, T 2024. Optimal Quantity Investigation of Metakaolin and Silica Fume in Production of Durable Acid Resistance Alkali Activated Slag Concrete. *Buildings* **14**(1), 21. doi: 10.3390/buildings14010021.
28. Szymczak-Graczyk, A, Garbowski, T and Ksit, B 2024. *Influence of geometric parameters on internal forces in the walls of rectangular tanks*. Proceedings of the 9th World Multidisciplinary Congress on Civil Engineering, Architecture and Urban Planning, Ostrava, Czech Republic, September 2-6, [in print].

29. Garbowski, T, Szymczak-Graczyk, A and Rutkowski, J 2024. *Optimization of Rectangular Tank Cross-Section Using Trust Region Gradient Method.* Proceedings of the 9th World Multidisciplinary Congress on Civil Engineering, Architecture and Urban Planning, Ostrava, Czech Republic, September 2-6, [in print].
30. MATLAB 2023b. *MATLAB version 9.14.0 (R2023b)*. Natick, Massachusetts: The MathWorks Inc.
31. Lee, J and Fenves, GL 1998. Plastic-Damage Model for Cyclic Loading of Concrete Structures. *Journal of Engineering Mechanics* **124**(8), 892–900.
32. Hillerborg, A, Modeer, M and Petersson, PE 1976. Analysis of Crack Formation and Crack Growth in Concrete by Means of Fracture Mechanics and Finite Elements. *Cement and Concrete Research* **6**, 773–782.
33. Lubliner, J, Oliver, J, Oller, S and Oñate, E 1989. A Plastic-Damage Model for Concrete. *International Journal of Solids and Structures* **25**, 299–329.
34. Ugray, Z, Lasdon, L, Plummer, J, Glover, F, Kelly, J and Martí, R 2007. Scatter Search and Local NLP Solvers: A Multistart Framework for Global Optimization. *INFORMS Journal on Computing* **19**(3), 328–340. doi: 10.1287/ijoc.1060.0175.
35. Neumaier, A 2004. Complete Search in Continuous Global Optimization and Constraint Satisfaction. *Acta Numerica* **13**, 271–369. doi: 10.1017/S0962492904000194.
36. Horst, R and Pardalos, PM 1995. *Handbook of Global Optimization*. Boston, MA: Springer. doi: 10.1007/978-1-4615-2025-2_20.